Continuous low-level dietary exposure to glyphosate elicits dose and sex-dependent synaptic and microglial adaptations in the rodent brain.

Noemie Cresto, Margot Courret, Athénaïs Génin, Céline Marie Pauline Martin, Julie Bourret, Sophie Sakkaki, Frederic de Bock, Alicia Janvier, Arnaud Polizzi, Laurence Payrastre, et al.

Continuous low-level dietary exposure to glyphosate elicits dose and sex-dependent synaptic and microglial adaptations in the rodent brain.

Noemie Cresto[1], Margot Courret[1], Athénaïs Génin[1], Céline Marie Pauline Martin[2], Julie Bourret[1], Sophie Sakkaki[1], Frederic de Bock[1], Alicia Janvier[1], Arnaud Polizzi[2], Laurence Payrastre[2], Sandrine Ellero-Simatos[2], Etienne Audinat[1], Julie Perroy[1], Nicola Marchi[1].

[1]Institute of Functional Genomics, University of Montpellier, CNRS, INSERM, Montpellier, France. [2]Toxalim (Research Centre in Food Toxicology), INRAE, ENVT, INP-Purpan, UPS, Université de Toulouse, Toulouse, France

Running title: Neuro-glial cell adjustments to dietary glyphosate.

Keywords: glyphosate, NOAEL, ADI, perinatal exposure, post-natal exposure, neuronal transmission, neuroglia.

Number of text pages: 37
Number of words: 3842
Number of figures: 5
Number of Supplemental Figures: 3
Number of Supplemental Tables: 1

Corresponding Authors:
Dr. Nicola Marchi, Cerebrovascular and Glia Research, Institut de Génomique Fonctionnelle (University of Montpellier, CNRS, INSERM), 141 rue de la Cardonille, 34094 Montpellier, Cedex 5, France. Email: nicola.marchi@igf.cnrs.fr.
Dr. Julie Perroy, Pathophysiology of synaptic transmission. Institut de Génomique Fonctionnelle (University of Montpellier, CNRS, INSERM), 141 rue de la Cardonille, 34094 Montpellier, Cedex 5, France. Email: julie.perroy@igf.cnrs.fr

Acknowledgment: This work was supported by ANR-Glyflore to LGP, SES, JP, and NM, ANR-Hepatobrain to NM, EnviroDisorders to JP, ANR-CEST-Focus, ANR-EpiCatcher to NM, ANR Microsenso to EA

ORCID Nicola Marchi: https://orcid.org/0000-0001-9124-0226

Abstract

Prolonged exposure to low levels of dietary contaminants is a context in modern life that could alter organ physiology gradually. Here, our objective was to investigate the impact of continuous exposure to acceptable daily intake (ADI) and non-observable adverse effect level (NOAEL) of glyphosate from gestation to adulthood using C57BL/6J mice and incorporating these levels into their food pellets. From adulthood, we analyzed neurophysiological and neuro-glia cellular adaptations in male and female animals.

Using ex-vivo hippocampal slice electrophysiology, we found a reduced efficacy of Schaffer collateral-to-CA1 excitatory synapses in glyphosate-exposed dietary conditions, with ADI and NOAEL dose-dependent effects. Short-term facilitation of excitatory synaptic transmission was specifically increased in NOAEL conditions, with a predominant influence in males, suggesting a reduced probability of neurotransmitter release. Long-term synaptic potentiation (LTP) was decreased in NOAEL-exposed mice. Next, we explore whether these neurophysiological modifications are associated with neuro-glia changes in the somatosensory cortex and hippocampus. High-resolution confocal microscopy analyses unveil a dose-dependent increased density of excitatory Vglut1^{+} Homer1^{+} synapses. Microglial Iba1^{+} cells displayed a shortening of their ramifications, a sign of cellular reactivity that was more pronounced in males at NOAEL levels. The morphology of GFAP^{+} astrocytes was not modified. Finally, we asked whether mouse-specific cross-correlations exist among all data sets generated. This examination included the novel object recognition (NOR) test from an open-field screening to which all mice were exposed before ex vivo functional and immunohistochemical examinations. We report a negative linear regression between

the number of synapses and NOR or LTP maintenance when plotting ADI and NOAEL datasets.

These results outline synaptic and microglial cell adaptations resulting from prenatal and continuous dietary low levels of glyphosate, discernible in, but not limited to, adult males exposed to the NOAEL. We discuss the significance of these findings to real-world consumer situations and long-term brain resilience.

Highlights

1) Dietary exposure to low glyphosate levels from prenatal to adulthood prompts neuro-glial adjustments.

2) In adults, synaptic function and number are modified mainly at NOAEL glyphosate compared to ADI.

3) Reduced microglial cell ramifications hint at activation, mainly at NOAEL dose.

4) These results hint at a dose-dependent vulnerability in the adult brain caused by dietary glyphosate.

Introduction

The possibility that environmental contaminants may pose risks to consumers' health is increasingly debated [1]. Given its extensive usage, glyphosate is under scrutiny due to its presence in numerous matrices, including human biofluids, making it a primary focus of investigation [2–4]. Regulatory bodies worldwide have granted glyphosate's approval for use; however, concerns regarding its impact on humans and the environment steadily mount [5].

Glyphosate was originally employed as an inhibitor of 5-enolpyruvylshikimate-3-phosphate synthase in plants [6]. From this initial framework, glyphosate was shown to impact bacteria, including within the microbiota [7], and other physiological functions, such as at the brain level [8]. Epidemiological studies have suggested a potential association between exposure to environmental contaminants, such as glyphosate, and neurodevelopmental risks [8], although controversy exists [9]. The hypothesis exists that glyphosate, as an aminophosphonic analog of the natural amino acid glycine, may directly influence synaptic transmission. Experimentally, screenings for neurological adaptations have been performed in settings where high glyphosate or glyphosate-based herbicides are administered and tested or over short periods [8 10–19]. More recently, a paradigm shift has emerged, involving consumer-relevant modalities for exposure to contaminants [20]. The latter involves testing, at a multi-organ level, the acceptable daily intake (ADI) or non-observable adverse effect level (NOAEL) of contaminants over extended periods [21–23].

To advance our understanding of this complex subject, and to specifically examine the impact of low-levels dietary glyphosate on the brain, we designed a protocol in which groups of C57BL/6J male and female mice were continuously exposed to glyphosate levels equivalent to ADI (0.5 mg/Kg body weight/day) and NOAEL (50 mg/Kg body weight/day) standards from the pre-natal to post-natal stages and compared to a control diet. We tested the hypothesis that dietary exposure to glyphosate could alter synaptic transmission in the mouse central nervous system. The selected read-outs represent fundamental biomarkers indicative of proper neuronal connectivity. Next, we used synaptic density and glial cell high-resolution imaging to study the existence of structural modifications. Finally, we correlate functional and histological read-outs with behavioral testing. Our results show the dose-dependent impacts induced by dietary exposure to glyphosate, particularly in male mice, where adaptations in synaptic transmission and density, as well as morphological changes in microglia, occurred. Whether these adjustments may determine a frail condition or impact brain resilience during adulthood is discussed.

Methods

Animals

All procedures were conducted by the Directive of the Council of the European Communities, supervised by the local animal welfare units, and approved by the French Ministry of Research (APAFIS # 16136 and APAFIS # 2020021914472552 # 24578 v3 at INRAE-Toxalim and IGF). Eight-week-old female and male C57BL/6J mice were purchased from Charles Rivers laboratories, allowed to acclimatize for one week, and fed a standard chow diet. Mice were housed in facilities under a 12 h light/12 h dark cycle (room temperature: 22±1°C), with *ad libitum* access to food and water. At Toxalim, nine male and eighteen female mice were randomly divided into 3 groups and fed control, ADI, or NOAEL diets for one week before mating. At mating, mice were housed 3 per cage (one male and two females) and fed the same diets as previously. After a mating period of 5 days (observation of a vaginal plug), the males were removed from the cages. At weaning, F1 males and females were separated and housed with 3-4 mice per cage according to their experimental group as detailed: n=12 control (CTR) males in 3 cages, n=12 ADI males in 3 cages, n=9 NOAEL males in 3 cages, n=8 CTR females in 2 cages, n=11 ADI females in 3 cages, n=16 NOAEL females in 5 cages. F1 mice were continuously fed the same diet as their parents. Body weight, general well-being, food, and water consumption were daily monitored. Tests (F1 from PN60, at IGF) were performed during the daily portion of the circadian rhythm (9 a.m. - 2 p.m.). To conform to the 3R rules, animals were used for consecutive exams (non-invasive behavioral explorations, ex-vivo hippocampal slice recording, and brain tissue histology; see Figure legends for specific numbers).

Glyphosate-containing pellets, dosage, and exposure protocol.

Glyphosate (Sigma-Aldrich) was solubilized in a mixture of methanol and acetone at a volume ratio of 9:1 (v/v). The glyphosate solution was evenly distributed onto the vitamin powder (PV 200, Scientific Animal Food Engineering; SAFE, Augy, France) and subsequently homogenized using a rotavapor (Laborota 4000™; BUCHI Switzerland). The homogenization process involved 30 minutes at 45 °C to evaporate the solvents, followed by an additional 50 minutes at room temperature. The control feed was prepared using the same procedure as described above, with the vitamin powder treated with a 9:1 mixture of methanol:acetone, excluding the addition of glyphosate. The vitamin powder, whether enriched with glyphosate or not, was sent to the Animal and Food Science Unit (SAAJ, Jouy en Josas, France) at the National Research Institute for Agriculture, Food and Environment (INRAE). They prepared control and glyphosate-enriched pellets by combining control or glyphosate-enriched vitamin powders (1%) with mineral supplements (7%) and other dietary constituents (63% carbohydrate, 5% fat, 22% protein, and 2% cellulose). Glyphosate quantification in the pellets was conducted by Eurofins (Nantes, France) using gas-chromatography–tandem mass spectrometry and liquid-chromatography–tandem mass spectrometry (ADI 1.7 mg/kg and NOAEL 170 mg/kg of pellet). Exposure levels were calculated based on the weekly annotations of food consumption and animal body weights (Supplemental Figure 1).

Behavioral screening.

We conducted a non-invasive open field (OF) assessment to measure locomotion (distance covered), time spent in the center arena (indicative of anxiety-like traits), and novel object recognition (working memory; NOR). Specifically, the animals were placed within a 50 cm x 45 cm open field (OF) arena. Locomotor activity in this setting provides both qualitative and quantitative biomarker indications of the animals' well-being and exploratory skills. The activity was captured and recorded over 10 minutes using the EthoVision XT15 video tracking system (Noldus in Wageningen, Netherlands). Following a 24-hour interval, mice underwent NOR testing, which serves as a quantitative measure of working memory. Initially, the mice were placed in the testing arena for 10 minutes, with two identical objects (transparent cylindrical; A and A'). The re-test trial occurred 24 hours later, during which object A was reintroduced alongside a new object B (opaque cubic), both positioned within the arena. The time (tA and tB) spent exploring the two objects was recorded. A recognition index (RI) was calculated as RI = tB / (tA + tB).

Ex-vivo electrophysiological recordings.

After rapid cervical dislocation, the right hippocampus was isolated and sectioned into 300 µm-thick slices in an ice-cold solution of artificial cerebrospinal fluid containing sucrose (aCSF sucrose composed in mM of 87 NaCl, 25 NaHCO3, 75 sucrose, 10 D-glucose, 2. 5 KCl, 1 NaH2PO4, 7 MgCl2 and oxygenated with carbogen (95% oxygen (O2) and 5% carbon dioxide (CO2)) using a vibratome (VT1200S, Leica, Bannockburn, IL, USA). The slices were stored at room temperature in a chamber

containing the cutting solution for 15 minutes before being transferred to a second chamber containing normal aCSF (119 NaCl, 26.2 NaHCO3, 11 D-glucose, 2.5 KCl, 1 NaH2PO4, 1.3 MgSO47H2O in mM and saturated with carbogen) heated to 34°C, for at least one hour before the first recording.

Slices were transferred to an immersed chamber mounted on a BX61 Olympus microscope to record extracellular field potentials. The slices were perfused with aCSF containing picrotoxin (100 µM) at 30-32°C at a flow rate of 1.5 ml/min by a peristaltic pump. A cut between CA3 and CA1 was made to avoid epileptiform activity. Glass pipettes, drawn with a horizontal puller (Sutter Instrument, Novato, CA, USA) and filled with aCSF, were used to stimulate the Schaffer collaterals of CA1. They were placed approximately 200 µm from the area where the evoked field excitatory postsynaptic potentials (fEPSPs) were recorded by a second glass pipette filled with aCSF and connected to the recording system. The fEPSPs were recorded and filtered (low-pass at 1 kHz) with an Axopatch 200 A amplifier (Axon Instruments, Union City, CA, USA), digitized at 10 kHz with an A/D converter (Digidata 1322 A, Axon Instruments), then stored and analyzed on a computer using Pclamp9 software (Molecular Devices, San Jose, CA, USA). Baseline evoked responses were monitored for 10 minutes, and only slices with stable fEPSP amplitudes were included. Input-output (I-O) relationships for fEPSPs were measured at the start of each experiment by applying a series of stimuli of increasing intensity to Schaffer's collaterals and plotting the initial slope of the fEPSP against the amplitude of the fiber volley. Paired-pulse facilitation (PPF) was evoked by administering two stimuli at a 40 ms interval and was measured by dividing the maximum amplitude of the second response by that of the first. Long-term potentiation

(LTP) was induced by tetanic stimulation of Schaffer collaterals (two trains of 100 Hz for 1 s, 20 s apart).

Synapse and glial cell analyses.

After brain isolation, the left hemisphere was placed in a 4% paraformaldehyde (PFA) solution for tissue fixation for 24 hours at 4°C. The following day, the PFA was replaced with phosphate-buffered saline (PBS) containing 30% sucrose for cryoprotection for 24 hours at 4°C. The left hemisphere was cut into 20 µm-thick slices using a cryostat (Leica, Germany). Slices were stored in cryoprotection buffer (30% water, ethylene glycol, glycerol, and 10% 1M tris buffer) at -20°C.

After three washes in PBS, the slices were blocked with a PBS-horse serum-Triton solution (PBS with 20% horse serum and 0.25% Triton) for 1h at room temperature, then incubated overnight at 4°C with the primary antibodies in the blocking solution. Antibodies against the glial acidic fibrillary protein (chicken GFAP antibody ab4674) and ionized calcium-bound adaptor molecule 1 (rabbit antibody IBA1 Wako 019-19741) were used to label astrocytes and microglia, respectively, for morphological analysis [24]. Antibodies against vesicular transporter 1 (Vglut1) and Homer protein homolog 1 (Homer1) were used to label pre- and post-synapses, respectively. The following day, slices were washed three times with PBS, incubated for 2h with secondary antibodies in blocking solution, and washed three times with PBS before mounting with Fluoromount containing DAPI (Invitrogen). For morphological analysis of microglia and astrocytes, z-stack images were acquired using an automated imaging system (Axioscan, Zeiss, Plateforme Montpellier Ressources

Imagerie) for morphological analysis at 20X. Astrocytes were selected based on GFAP and microglia on IBA1 labeling. After cell isolation, the 8-bit images were first filtered (unsharp mask process set to 2.0 radius and 0.9 mask weight) and adjusted using Triangle thresholding (min = 175 and max = 255). The ImageJ 'Sholl analysis' plugin was then used to assess cell branching [25]. It consists of applying concentric circles from the center of the cell soma spaced 5 µm apart. Each intersection between the GFAP labeling for astrocytes or IBA1 for microglia and the circle is counted to assess the amount of cell extension. For synapse analyses, images were acquired with a confocal microscope (Zeiss Airyscan, Plateforme Montpellier Ressources Imagerie) using a 63X oil immersion objective (image size: 103.10 x 103.10 µm, Resolution x,y: 140 nm; z: 450 nm). Two regions of interest in two sections were acquired per animal. For each section, in both channels (488 nm and 633 nm), we imaged serial optical sections at 0.17 µm intervals over a total of 5 µm for 30 optical sections. For image analysis, automated quantification was performed using the Distance Analysis plugin (DiAna)[26]. The plugin performs automated object-based co-localization and distance analysis in 3D. As the first step, we used the global intensity thresholding (median) to select dots in each channel corresponding to Vglut1 and Homer1. This step created a new image for each channel representing each dot. Then, the plugin evaluates the co-localization between the dots of each channel. Co-localized signals were considered synapses, and the number of synapses was automatically calculated. Results were expressed in the number of synapses per 100 μm^3.

Statistical analyses.

GraphPad Prism (La Jolla, California) was used. The normality of all the data was tested using the Shapiro-Wilk test. The one-factor or two-factor ANOVA mean comparison test was then performed for data that followed a normal distribution, and the Kruskal-Wallis test for data that did not follow a normal distribution. Multiple comparisons were computed using the Bonferonni posthoc test for ANOVAs and Dunn's posthoc test for Kruskal-Wallis. A group T-test was performed on the object recognition test data to check that the scores differed from the theoretical value, i.e., a discrimination ratio 0.5 corresponding to an identical exploration of the two objects. Multiple correlations and graphical representations were generated using R software. Symbols indicate statistical significance (* $p<0.05$; ** $p<0.01$; *** $p<0.001$; **** $p<0.0001$); *: CTR vs NOAEL; $: ADI vs NOAEL; #: CTR vs ADI; ns: not significant. Supplemental Table 1 provides details of statistical analyses computed for all experiments.

Results

Dietary glyphosate is associated with adaptations in synaptic transmission and long-term potentiation during adulthood.

In our experimental settings, mice did not exhibit significant differences in food consumption, except for isolated time points in males fed NOAEL glyphosate (Supplemental Figure 2C-D). Body weight was reduced (~10%) long-term in male mice fed with NOAEL glyphosate pellets (Supplemental Figure 2A-B). In these groups, and following behavioral testing (see below), we investigated whether synaptic-level modifications ensue due to dietary glyphosate. First, to interrogate synaptic strength, we evaluated basal evoked synaptic transmission at CA1 Schaffer collateral synapses in acute hippocampal slices from adult mice (Figure 1A). We confirm that non-exposed mice had normal excitatory synaptic transmission by comparing the amplitude of the presynaptic fiber volley (input) to the slope of the excitatory field potential (fEPSP; output) [27]. In contrast, in the glyphosate-exposed groups, the excitatory synaptic efficacy decreased significantly by ~50% and ~30% in the NOAEL and ADI conditions, respectively, and compared to control (Figure 1C). We segregated females (Figure 1D) and males (Figure 1E), confirming the effects of NOAEL glyphosate on both sexes. We further investigated the presence of presynaptic alterations by assessing paired-pulse facilitation (PPF), a form of short-term plasticity sensitive to changes in presynaptic release probability (Figure 1B). Consistent with the intact basal synaptic transmission, we found a paired-pulse ratio (PPR) approaching 1.5 in non-exposed mice. In ADI-exposed mice, the PPR was similar to the control, while it increased in NOAEL conditions (Figure 1F), suggesting a reduced probability of release at schaffer

collateral terminals. Figure 1G-H shows the patterns of sex-specific modifications, with effects significant in males.

Because glyphosate exposure reduces the efficacy of CA1 Schaffer collateral synapses in adult mice, we next investigated its impact on long-term synaptic plasticity (Figure 2A). We found that the magnitude of LTP, induced by brief tetanic stimulation of Schaffer collaterals, was reduced by ~30% in NOAEL-exposed mice (Figure 2B and 2E) compared to non-exposed condition. The ADI exposition did not alter the LTP. Figure 2C-D and Figure 2F-G show the patterns of sex-specific modifications. Male mice generally presented the most significant modifications (Figures 1 and 2). See Supplemental Table 1 for complete statistical analyses. Together, these results indicate the existence of synaptic defects, particularly in male mice continuously exposed to dietary NOAEL glyphosate.

Dietary glyphosate is associated with increased synaptic density.

Next, we evaluate whether an alteration in the number of synapses accompanies the observed electrophysiological modifications. Using high-resolution imaging, we quantified the number of excitatory synapses in the hippocampus of adult mice exposed to glyphosate. Synapses were labeled with pre- and post-synaptic markers, Vglut1 and Homer1 (Figure 3A). The co-localization between Vglut1 and Homer1 was measured, with two co-localized dots indicating one synapse. The density of excitatory synapses increased in the glyphosate-exposed groups (Figure 3B). Sex-dependent data are shown in Figure 3C-D. Taken together, these data indicate that

continuous glyphosate exposure leads to functional and histological synapse modifications in a dose and sex-dependent manner.

Impact of glyphosate exposure on the morphology of astrocytes and microglial cells.

Accumulating evidence indicates the participation of glial cells in synaptic maturation and remodeling in health and disease [28]. Previous evidence showed that, in mice, glyphosate ingestion triggers neuroinflammatory changes, although evidence refers to high-level exposures [29,30]. Here, we examined the microglia and astrocyte histological alterations possibly associated with ADI and NOAEL glyphosate in males and females. We utilized Sholl's analysis and found that exposure to NOAEL-glyphosate was associated with decreased ramifications of Iba1+ microglia in the somatosensory parietal cortex and hippocampus (Figure 4C-D). This modification, observed in female and male mice (Figure 4F-G and I-J), hints at cellular activation. ADI-glyphosate had a negligible impact on microglial cells (Figure 4F-G and I-J). The analysis of GFAP+ astrocytes (Figure 4B) did not reveal significant morphological modifications associated with glyphosate exposure (Figure 4E-H), except for moderate cell remodeling in male mice under ADI conditions (Figure 4K). See Supplemental Table 1 for complete statistical analyses.

Cross-correlations between individual-specific read-outs.

Because functional synaptic and histological examinations were performed in a mouse-specific manner, we tested whether correlations exist among the data sets. In this analysis, we also integrated mouse-specific results from OF and NOR tests

conducted before the electrophysiological assessments. With this specific behavioral test setting, male and female mice did not show locomotor deficits (Supplemental Figure 3A-D) or anxiety-like traits (Supplemental Figure 3E-G) as the time spent at the center of the OM was unchanged after dietary glyphosate exposure. Mice exposed to NOAEL glyphosate exhibited a significant decrease in discrimination ratio (Figure 5A-D), a biomarker of spatial memory changes. When cross-correlating all results, we found a negative linear regression between the number of synapses and NOR or LTP maintenance in ADI and NOAEL-exposed animals (Figure 5E-F). These results suggest the presence of an increased number of non-fully functional synapses under NOAEL conditions. Furthermore, a trend correlation existed between NOR score and basal synaptic transmission in NOAEL-exposed animals (Figure 5G), although two outliers were present. A correlation matrix summarises trends and significant correlations between histological and functional hippocampal-associated read-outs obtained in a mouse-specific manner (Figure 5H).

Discussion

There is considerable debate regarding whether glyphosate adversely affects brain health and physiological function. Our findings indicate that continuous dietary exposure to low-level glyphosate levels from prenatal stages through adulthood can adjust synaptic transmission performance in a mouse model. At the cellular level, the increased synaptic density and histological indicators of microglial cell reactivity were concomitant to the electrophysiological changes. The NOAEL dose elicited most adaptations, predominantly in, but not limited to, adult males. The effect of ADI levels was more constrained, albeit discernable for selected read-outs. Taken together, these data may imply the potential for brain vulnerability associated with persistent low-level glyphosate exposure [23]. We should further investigate the functional relevance of the observed neuronal and microglial changes, especially considering their potential role across brain diseases. [31–33].

Glyphosate dosages and exposure duration: existing evidence.

The majority of existing experimental evidence is based on exposure protocols involving high doses of glyphosate and its commercially available formulations, such as glyphosate-based herbicides (GBH). Because GBH contain polyethylene tallow amine (POEA)-based surfactants and heavy metals, a current question is whether glyphosate alone or in combinations with adjuvants display similar or diverse patterns of toxicity [34]. In rodents, GBH negatively impacted neuronal transmission and behavioral outputs [14,35]. Maternal exposure to GBH at high levels induced autistic-like deficiencies in male offspring [36]. Glyphosate or GBH exposure has been reported to

cause perturbations in neurodevelopmental processes, leading to long-term neurophysiological changes in animal models [37–40]. At doses of 250 or 500 mg/kg GBH, offspring showed behavioral changes [12]. Both glyphosate and GBH were shown to cause disruption of neurogenesis accompanied by compensatory responses, modifying synaptic plasticity in the hippocampus [40]. Exposure to GBH leads to glutamate excitotoxicity, oxidative damage, and astrocyte dysfunction in offspring hippocampus [14]. TNF-alpha increased brain levels were reported in mice pre-natally exposed to GBH 0.3 mg/Kg [30].

Recent studies have started unveiling the impact of low-level dietary glyphosate on neurophysiological functions. At NOAEL levels, varying anxiety-like outcomes were reported [21,23]. We did not find changes in the time spent in the center of an OF arena, while others reported anxiety-like traits in females with NOAEL continuous exposure [23]. Sex-dependent modifications in social preference were found to result from NOAEL dietary exposure[21]. Assessing memory using novel object recognition, we previously found that male mice are not affected by NOAEL glyphosate exposure [41]. For this present study, we changed the experimental paradigm by increasing the time before each test session, thus exploring long-term memory. Here, a negative correlation existed between the number of synapses and NOR or LTP maintenance in NOAEL glyphosate-exposed animals (Fig. 5E-F), suggesting synaptic dysfunction. In accordance with our results, NOAEL glyphosate exposure during a critical period of neurodevelopment negatively impacted synaptic organization in the hippocampus with learning and memory deficits [12].

How can glyphosate impact the brain?

Varying glyphosate levels can be found in human body fluids, such as urine or amniotic fluids [42], and high-exposure intoxications can occur [43,44]. Glyphosate was reported to cross the placental and blood-brain barrier, events that could favor neurodevelopmental modifications [45–47]. Perinatal glyphosate exposure was linked with a risk of developing attention deficit and hyperactivity disorders in children, with a possible negative impact if parents were previously exposed [48 49].

As working hypotheses, exposure to glyphosate could trigger peripherally-mediated (e.g., immune responses [45] or modified microbiota within a gut-brain axis [50,51]) or direct damage to the brain borders and cerebrovascular permeability [22]. Importantly, microbiota adaptations were reported in mice continuously exposed to NOAEL and ADI dietary glyphosate, suggesting a scenario of a dysregulated gut-brain axis [23]. Our results revealed cellular adjustments in the brain, although we did not delve into specific mechanisms [5,8]. We identify microglial cells as sensitive to glyphosate, showing histological signs of cell reactivity in adults, along with an increased density and decreased efficacy of excitatory synapses. It is essential to understand the causal relationship between these multi-cellular events, including tracking how these changes may unfold. Microglial cells contribute to brain synapse remodeling during development, health, and disease [52–55]. Their function is fundamental for synaptic maturation and establishing functional circuits [56]. Our data, including the observed sex-dependent effects of glyphosate exposure, align with this framework. Future studies should test the hypothesis that microglia reactivity due to glyphosate exposure drives abnormal trajectories of synapse development.

Study Limitations and Conclusions.

Here, it is important to highlight that the majority of adaptations were observed in males subjected to continuous, daily exposure to NOAEL glyphosate levels, a scenario that exaggerates most consumer settings. Importantly, at ADI glyphosate levels, we observed some alterations in specific synaptic transmission measures and density. Drawing precise conclusions about the actual pathological significance of these changes presents a challenge. We suggest the hypothesis of a vulnerable, frail brain condition associated with this contaminant. This notion may gain significance in the context of pre-existing or acute pathological settings, such as genetic brain disorders or head trauma, leading to a dual-hit framework. Furthermore, the presented study leaves several unanswered questions and the possibility for further investigation. For instance, regional and temporal transcript analyses could unveil signatures indicating a frail condition, supported by the notion that glial cells critically contribute to controlling neuronal transmission in health and disease [28]. Similar reasoning applies to neurons, as we found synaptic adaptations using ex-vivo electrophysiology. Importantly, glyphosate and its major metabolite, aminomethylphosphonic acid (AMPA), have structural similarities to glycine and glutamate, respectively. The possibility exists for glyphosate to bind to the glycine or glutamate NMDA receptor binding pockets, impacting learning and memory controlled by this receptor. Glyphosate could reduce glutamate uptake and metabolism from glial cells [13] and modify brain monoaminergic neurotransmitter levels in rodents [19]. These scenarios need to be investigated. Next, *in vivo* electrophysiology should be performed primarily based on the ex-vivo analysis and modifications presented herein [57]. Finally, we examined only a limited number of behavioral parameters. This choice was dictated by

the high number of groups and the subsequence performance of *ex-vivo* neurophysiology and cell examinations on the same mice.

In summary, low-level glyphosate, when delivered through the diet and daily from pre-natal stages to adulthood, modifies distinct parameters of synaptic transmission and neuro-microglial cell structures. These adjustments support the notion of a frail, sex-specific condition that may unfavorably impact brain resilience over time [22 38].

Declaration of interests

The authors declare that they have no known competing financial interests or personal relationships that could have appeared to influence the work reported in this paper.

Bibliography

1. Kim, K.-H., Kabir, E. & Jahan, S. A. Exposure to pesticides and the associated human health effects. *Sci. Total Environ.* **575**, 525–535 (2017).
2. Myers, J. P. *et al.* Concerns over use of glyphosate-based herbicides and risks associated with exposures: a consensus statement. *Environ. Health Glob. Access Sci. Source* **15**, 19 (2016).
3. Niemann, L., Sieke, C., Pfeil, R. & Solecki, R. A critical review of glyphosate findings in human urine samples and comparison with the exposure of operators and consumers. *J. Für Verbraucherschutz Leb.* **10**, 3–12 (2015).
4. Van Bruggen, A. H. C. *et al.* Environmental and health effects of the herbicide glyphosate. *Sci. Total Environ.* **616–617**, 255–268 (2018).
5. Madani, N. A. & Carpenter, D. O. Effects of glyphosate and glyphosate-based herbicides like Roundup™ on the mammalian nervous system: A review. *Environ. Res.* **214**, 113933 (2022).
6. Schönbrunn, E. *et al.* Interaction of the herbicide glyphosate with its target enzyme 5-enolpyruvylshikimate 3-phosphate synthase in atomic detail. *Proc. Natl. Acad. Sci. U. S. A.* **98**, 1376–1380 (2001).
7. Mao, Q. *et al.* The Ramazzini Institute 13-week pilot study on glyphosate and Roundup administered at human-equivalent dose to Sprague Dawley rats: effects on the microbiome. *Environ. Health* **17**, 50 (2018).
8. Costas-Ferreira, C., Durán, R. & Faro, L. R. F. Toxic Effects of Glyphosate on the Nervous System: A Systematic Review. *Int. J. Mol. Sci.* **23**, 4605 (2022).
9. Chang, E. T., Odo, N. U. & Acquavella, J. F. Systematic literature review of the epidemiology of glyphosate and neurological outcomes. *Int. Arch. Occup. Environ. Health* **96**, 1–26 (2023).
10. Bali, Y. A., Kaikai, N.-E., Ba-M'hamed, S. & Bennis, M. Learning and memory impairments associated to acetylcholinesterase inhibition and oxidative stress following glyphosate based-herbicide exposure in mice. *Toxicology* **415**, 18–25 (2019).
11. Ait Bali, Y., Ba-Mhamed, S. & Bennis, M. Behavioral and Immunohistochemical Study of the Effects of Subchronic and Chronic Exposure to Glyphosate in Mice. *Front. Behav. Neurosci.* **11**, 146 (2017).
12. Ait-Bali, Y. *et al.* Pre- and postnatal exposure to glyphosate-based herbicide causes behavioral and cognitive impairments in adult mice: evidence of cortical ad hippocampal dysfunction. *Arch. Toxicol.* **94**, 1703–1723 (2020).
13. Cattani, D. *et al.* Mechanisms underlying the neurotoxicity induced by glyphosate-based herbicide in immature rat hippocampus: involvement of glutamate excitotoxicity. *Toxicology* **320**, 34–45 (2014).
14. Cattani, D. *et al.* Developmental exposure to glyphosate-based herbicide and depressive-like behavior in adult offspring: Implication of glutamate excitotoxicity and oxidative stress. *Toxicology* **387**, 67–80 (2017).
15. Coullery, R., Pacchioni, A. M. & Rosso, S. B. Exposure to glyphosate during pregnancy induces neurobehavioral alterations and downregulation of Wnt5a-CaMKII pathway. *Reprod. Toxicol. Elmsford N* **96**, 390–398 (2020).
16. Hernández-Plata, I., Giordano, M., Díaz-Muñoz, M. & Rodríguez, V. M. The herbicide glyphosate causes behavioral changes and alterations in dopaminergic markers in male Sprague-Dawley rat. *Neurotoxicology* **46**, 79–91 (2015).
17. Ji, H., Xu, L., Wang, Z., Fan, X. & Wu, L. Differential microRNA expression in the prefrontal cortex of mouse offspring induced by glyphosate exposure during pregnancy and lactation. *Exp. Ther. Med.* **15**, 2457–2467 (2018).

18. Luna, S., Neila, L. P., Vena, R., Borgatello, C. & Rosso, S. B. Glyphosate exposure induces synaptic impairment in hippocampal neurons and cognitive deficits in developing rats. *Arch. Toxicol.* **95**, 2137–2150 (2021).
19. Martínez, M.-A. *et al.* Neurotransmitter changes in rat brain regions following glyphosate exposure. *Environ. Res.* **161**, 212–219 (2018).
20. Bicca, D. F., Spiazzi, C. C., Ramalho, J. B., Soares, M. B. & Cibin, F. W. S. A subchronic low-dose exposure of a glyphosate-based herbicide induces depressive and anxious-like behavior in mice: quercetin therapeutic approach. *Environ. Sci. Pollut. Res. Int.* **28**, 67394–67403 (2021).
21. Del Castilo, I. *et al.* Lifelong Exposure to a Low-Dose of the Glyphosate-Based Herbicide RoundUp® Causes Intestinal Damage, Gut Dysbiosis, and Behavioral Changes in Mice. *Int. J. Mol. Sci.* **23**, 5583 (2022).
22. Cresto, N. *et al.* Pesticides at brain borders: Impact on the blood-brain barrier, neuroinflammation, and neurological risk trajectories. *Chemosphere* **324**, 138251 (2023).
23. Buchenauer, L. *et al.* Maternal exposure of mice to glyphosate induces depression- and anxiety-like behavior in the offspring via alterations of the gut-brain axis. *Sci. Total Environ.* **905**, 167034 (2023).
24. Dincã, D. M. *et al.* Myotonic dystrophy RNA toxicity alters morphology, adhesion and migration of mouse and human astrocytes. *Nat. Commun.* **13**, 3841 (2022).
25. Ferreira, T. A. *et al.* Neuronal morphometry directly from bitmap images. *Nat. Methods* **11**, 982–984 (2014).
26. Gilles, J.-F., Dos Santos, M., Boudier, T., Bolte, S. & Heck, N. DiAna, an ImageJ tool for object-based 3D co-localization and distance analysis. *Methods San Diego Calif* **115**, 55–64 (2017).
27. Cresto, N. *et al.* Hippocampal Excitatory Synaptic Transmission and Plasticity Are Differentially Altered during Postnatal Development by Loss of the X-Linked Intellectual Disability Protein Oligophrenin-1. *Cells* **11**, 1545 (2022).
28. Rasband, M. N. Glial Contributions to Neural Function and Disease *. *Mol. Cell. Proteomics* **15**, 355–361 (2016).
29. Winstone, J. K. *et al.* Glyphosate infiltrates the brain and increases pro-inflammatory cytokine TNFα: implications for neurodegenerative disorders. *J. Neuroinflammation* **19**, 193 (2022).
30. de Castro Vieira Carneiro, C. L. *et al.* Behavioral and neuroinflammatory changes caused by glyphosate: Base herbicide in mice offspring. *Birth Defects Res.* **115**, 488–497 (2023).
31. Muzio, L., Viotti, A. & Martino, G. Microglia in Neuroinflammation and Neurodegeneration: From Understanding to Therapy. *Front. Neurosci.* **15**, (2021).
32. Klement, W. *et al.* Seizure progression and inflammatory mediators promote pericytosis and pericyte-microglia clustering at the cerebrovasculature. *Neurobiol. Dis.* **113**, 70–81 (2018).
33. Di Nunzio, M. *et al.* Microglia proliferation plays distinct roles in acquired epilepsy depending on disease stages. *Epilepsia* **62**, 1931–1945 (2021).
34. Mesnage, R., Bernay, B. & Séralini, G.-E. Ethoxylated adjuvants of glyphosate-based herbicides are active principles of human cell toxicity. *Toxicology* **313**, 122–128 (2013).
35. Gallegos, C. E. *et al.* Exposure to a glyphosate-based herbicide during pregnancy and lactation induces neurobehavioral alterations in rat offspring. *Neurotoxicology* **53**, 20–28 (2016).

36. Pu, Y. *et al.* Glyphosate exposure exacerbates the dopaminergic neurotoxicity in the mouse brain after repeated administration of MPTP. *Neurosci. Lett.* **730**, 135032 (2020).
37. Ruuskanen, S., Rainio, M. J., Uusitalo, M., Saikkonen, K. & Helander, M. Effects of parental exposure to glyphosate-based herbicides on embryonic development and oxidative status: a long-term experiment in a bird model. *Sci. Rep.* **10**, 6349 (2020).
38. Forner-Piquer, I. *et al.* Differential impact of dose-range glyphosate on locomotor behavior, neuronal activity, glio-cerebrovascular structures, and transcript regulations in zebrafish larvae. *Chemosphere* **267**, 128986 (2021).
39. de Oliveira, M. A. L. *et al.* Perinatal exposure to glyphosate-based herbicides induced neurodevelopmental behaviors impairments and increased oxidative stress in the prefrontal cortex and hippocampus in offspring. *Int. J. Dev. Neurosci. Off. J. Int. Soc. Dev. Neurosci.* **82**, 528–538 (2022).
40. Ojiro, R. *et al.* Comparison of the effect of glyphosate and glyphosate-based herbicide on hippocampal neurogenesis after developmental exposure in rats. *Toxicology* **483**, 153369 (2023).
41. Sakkaki, S. *et al.* Dual-Hit: Glyphosate exposure at NOAEL level negatively impacts birth and glia-behavioural measures in heterozygous shank3 mutants. *Environ. Int.* **180**, 108201 (2023).
42. Ongono, J. S., Béranger, R., Baghdadli, A. & Mortamais, M. Pesticides used in Europe and autism spectrum disorder risk: can novel exposure hypotheses be formulated beyond organophosphates, organochlorines, pyrethroids and carbamates? - A systematic review. *Environ. Res.* **187**, 109646 (2020).
43. Gillezeau, C. *et al.* The evidence of human exposure to glyphosate: a review. *Environ. Health Glob. Access Sci. Source* **18**, 2 (2019).
44. Soukup, S. T. *et al.* Glyphosate and AMPA levels in human urine samples and their correlation with food consumption: results of the cross-sectional KarMeN study in Germany. *Arch. Toxicol.* **94**, 1575–1584 (2020).
45. von Ehrenstein, O. S. *et al.* Prenatal and infant exposure to ambient pesticides and autism spectrum disorder in children: population based case-control study. *BMJ* **364**, l962 (2019).
46. Martinez, A. & Al-Ahmad, A. J. Effects of glyphosate and aminomethylphosphonic acid on an isogeneic model of the human blood-brain barrier. *Toxicol. Lett.* **304**, 39–49 (2019).
47. Poulsen, M. S., Rytting, E., Mose, T. & Knudsen, L. E. Modeling placental transport: correlation of in vitro BeWo cell permeability and ex vivo human placental perfusion. *Toxicol. Vitro Int. J. Publ. Assoc. BIBRA* **23**, 1380–1386 (2009).
48. de Araujo, J. S. A., Delgado, I. F. & Paumgartten, F. J. R. Glyphosate and adverse pregnancy outcomes, a systematic review of observational studies. *BMC Public Health* **16**, 472 (2016).
49. Arcury, T. A. *et al.* Pesticide Exposure among Latinx Children in Rural Farmworker and Urban Non-Farmworker Communities: Associations with Locality and Season. *Int. J. Environ. Res. Public. Health* **20**, 5647 (2023).
50. Rueda-Ruzafa, L., Cruz, F., Roman, P. & Cardona, D. Gut microbiota and neurological effects of glyphosate. *Neurotoxicology* **75**, 1–8 (2019).
51. Walsh, L., Hill, C. & Ross, R. P. Impact of glyphosate (RoundupTM) on the composition and functionality of the gut microbiome. *Gut Microbes* **15**, 2263935.

52. Kettenmann, H., Kirchhoff, F. & Verkhratsky, A. Microglia: New Roles for the Synaptic Stripper. *Neuron* **77**, 10–18 (2013).
53. Frost, J. L. & Schafer, D. P. Microglia: Architects of the Developing Nervous System. *Trends Cell Biol.* **26**, 587–597 (2016).
54. Mosser, C.-A., Baptista, S., Arnoux, I. & Audinat, E. Microglia in CNS development: Shaping the brain for the future. *Prog. Neurobiol.* **149–150**, 1–20 (2017).
55. Thion, M. S. & Garel, S. Microglial ontogeny, diversity and neurodevelopmental functions. *Curr. Opin. Genet. Dev.* **65**, 186–194 (2020).
56. Thion, M. S. *et al.* Microbiome Influences Prenatal and Adult Microglia in a Sex-Specific Manner. *Cell* **172**, 500-516.e16 (2018).
57. Forner-Piquer, I. *et al.* Varying modalities of perinatal exposure to a pesticide cocktail elicit neurological adaptations in mice and zebrafish. *Environ. Pollut.* **278**, 116755 (2021).

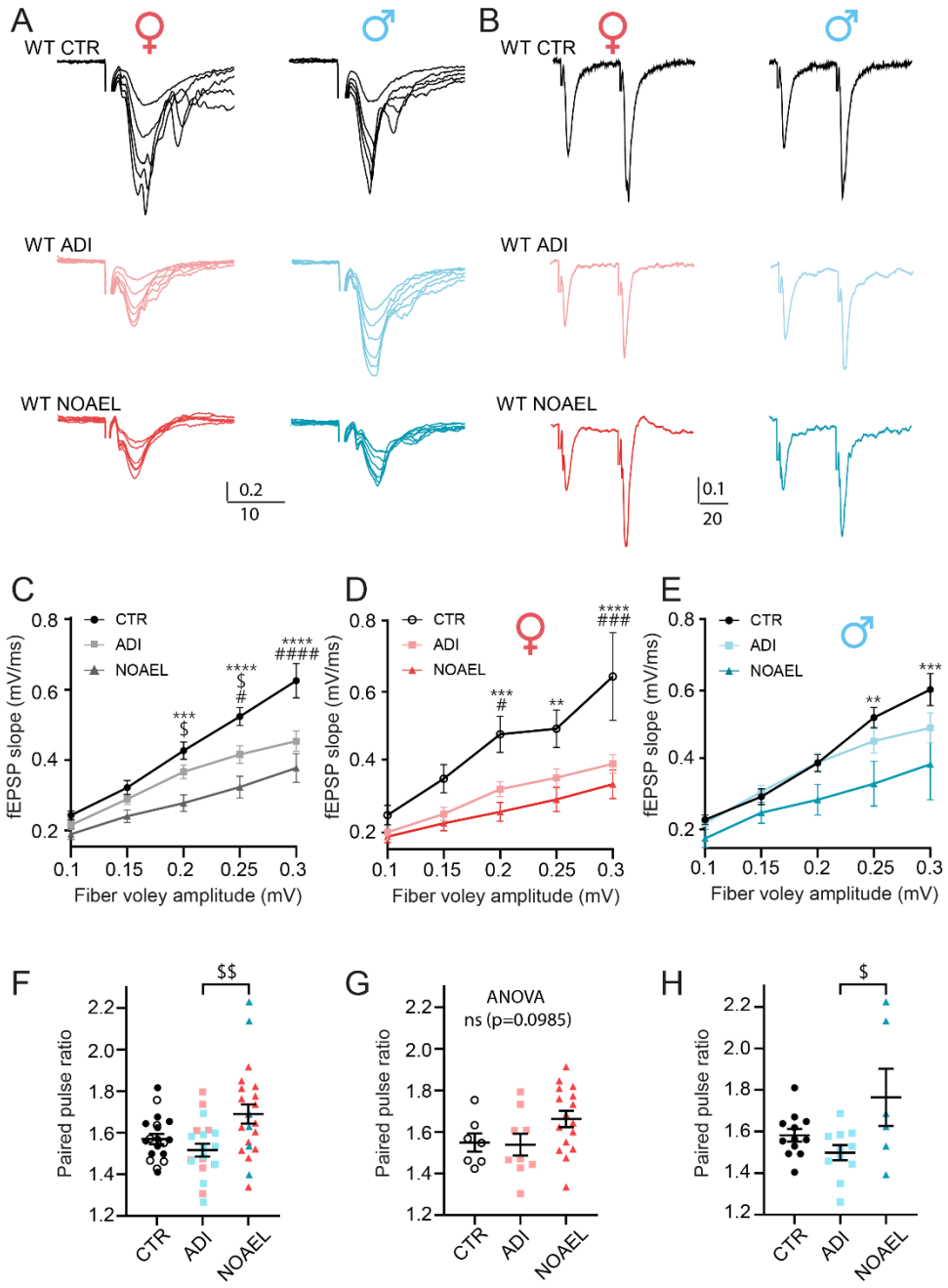

Figure 1. Basal excitatory synaptic transmission is reduced in the adult brain of ADI and NOAEL glyphosate-exposed mice. (A, C to E) The input/output curve shows that basal excitatory synaptic transmission at CA1 Schaffer collateral synapses is reduced in glyphosate-treated groups, males and females pooled **(C)**. Males CTR, n=14 ; ADI, n=11 ; NOAEL, n=6; Females CTR, n=6 ; ADI, n=8 ; NOAEL, n=13. Two-way ANOVA test (Males: p<0.0001; Females: p<0.0001; Males and Females: p<0.0001). **(B, F to H)** Paired-pulse facilitation (PPF) is increased in NOAEL glyphosate-treated mice, males, and females pooled **(F),** females **(G)**, and males **(H)**. Males CTR, n=12 ; ADI, n=11 ; NOAEL, n=6 ; Females CTR, n=7 ; ADI, n=9 ; NOAEL, n=16. One-way ANOVA test (Males: p=0.0236; Females: p=0.0985; Males and Females: p=0.0033). Asterisks indicate statistical significance (* p < 0.05; ** p < 0.01; *** p < 0.001; **** p < 0.0001) ; *: CTR vs NOAEL ; $: ADI vs NOAEL ; #: CTR vs ADI ; ns: non-significative.

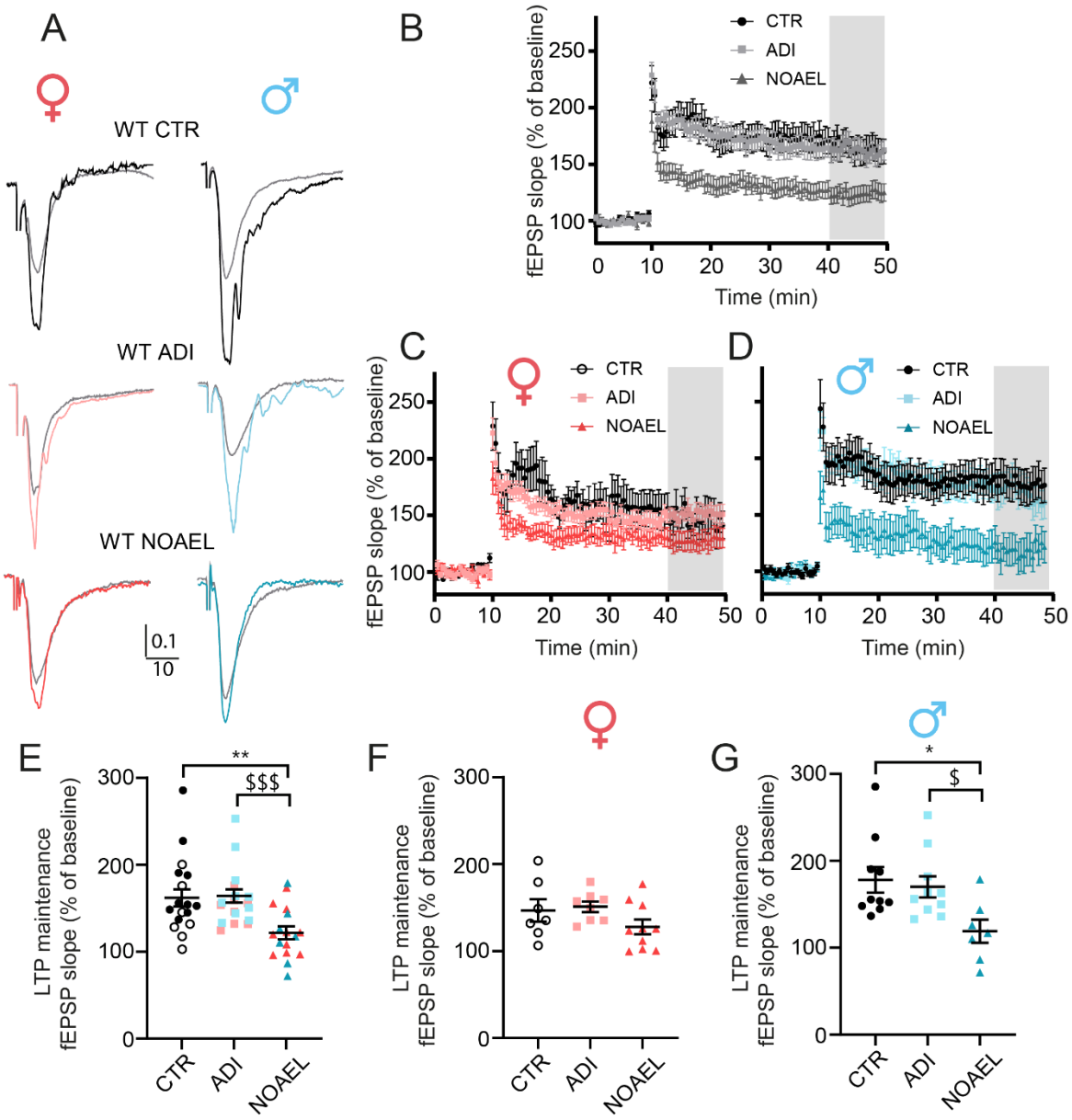

Figure 2. Long-term potentiation in the adult brain is reduced in NOAEL glyphosate exposure conditions. In all mice groups, LTP was measured by field potential recordings (fEPSPs) at CA1 Schaffer collateral synapses. The light gray box highlights the last 10 min of the recording used to calculate the LTP maintenance (50–60 min). **(A-D)**. Average fEPSPs after the tetanus were normalized to baseline values before high-frequency stimulation. Reduced LTP was observed in the NOAEL-exposed group. **(E-G)** The histograms represent the mean normalized fEPSP slope measured during the last 10 min of the recording, as indicated by the light gray box in B. LTP was affected in NOAEL groups compared to non-exposed mice. Males CTR, n=10 slices from 10 mice; ADI, n=10 slices from 10 mice; NOAEL, n=7 slices from 6 mice; Females CTR, n=7 slices from 5 mice; ADI, n=8 slices from 8 mice; NOAEL, n=10 slices from 9 mice. Kruskal-Wallis test (Males: p=0.0109); One-way ANOVA (Females: p=0.1657) and Kruskal wallis test (Males and Females: p=0.0003). Sample traces represent averaged field potentials before (light blue and light red) and 50–60 min after tetanization (dark blue and dark red). Asterisks indicate statistical significance (* $p < 0.05$; ** $p < 0.01$; *** $p < 0.001$; **** $p < 0.0001$) ; *: CTR vs NOAEL ; $: ADI vs NOAEL ; #: CTR vs ADI ; ns: non-significative.

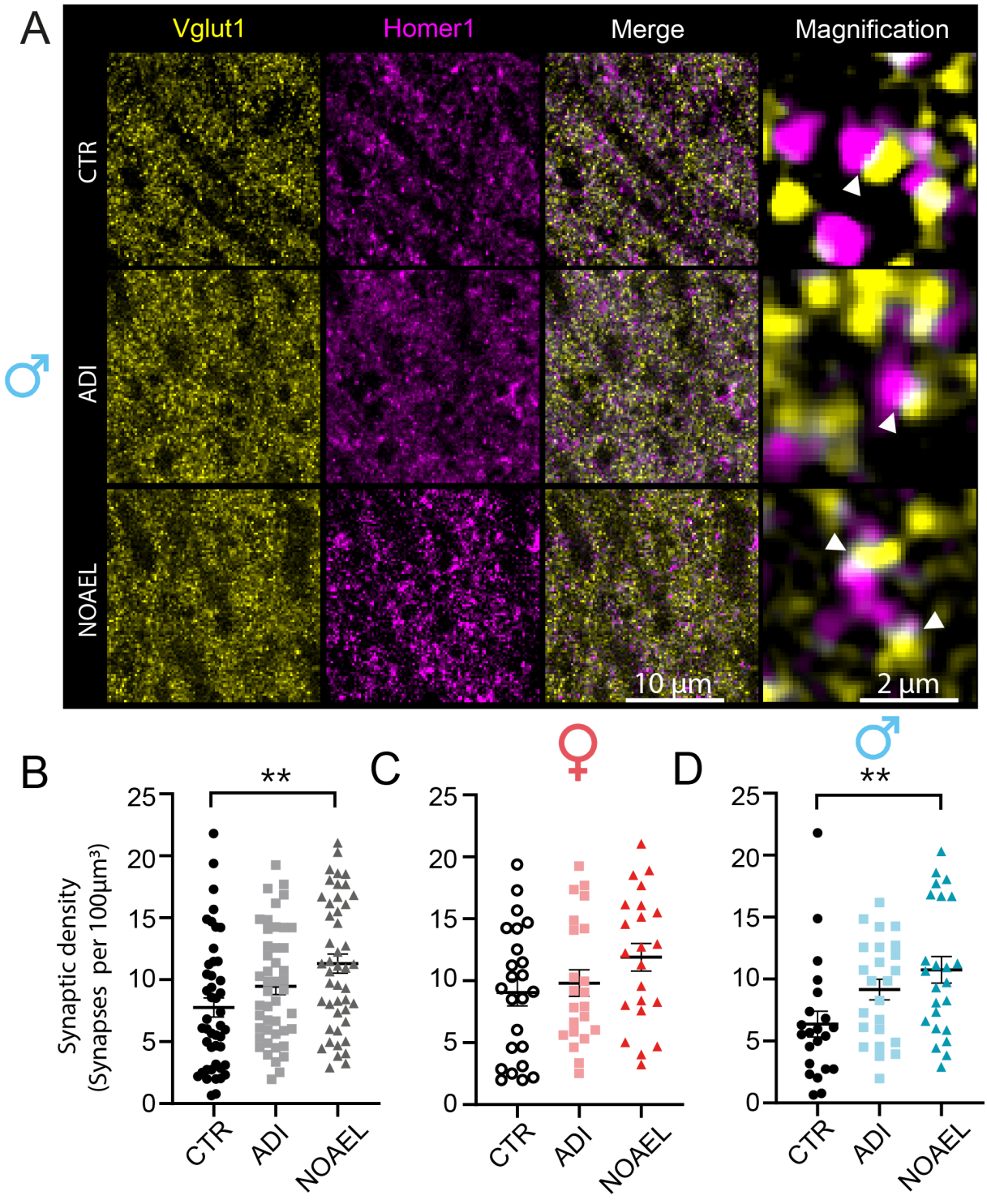

765

766 **Figure 3. NOAEL exposure induces an increase in excitatory synapses in adult mice.**
767 **(A)** Representative images (males) of excitatory synapses labeled with Vglut1 (yellow) and
768 Homer1 (magenta), co-localized dots (white, marked with arrows) identified one synapse. **(B)**
769 Synaptic density, **(C)** synaptic density in females, and **(D)** in males (CTR: n = 22 ROI from n =
770 6 mice, DJA: n = 24 ROI from n = 6 mice, NOAEL: n = 24 ROI from n = 6). Asterisks indicate
771 statistical significance (** $p < 0.01$).

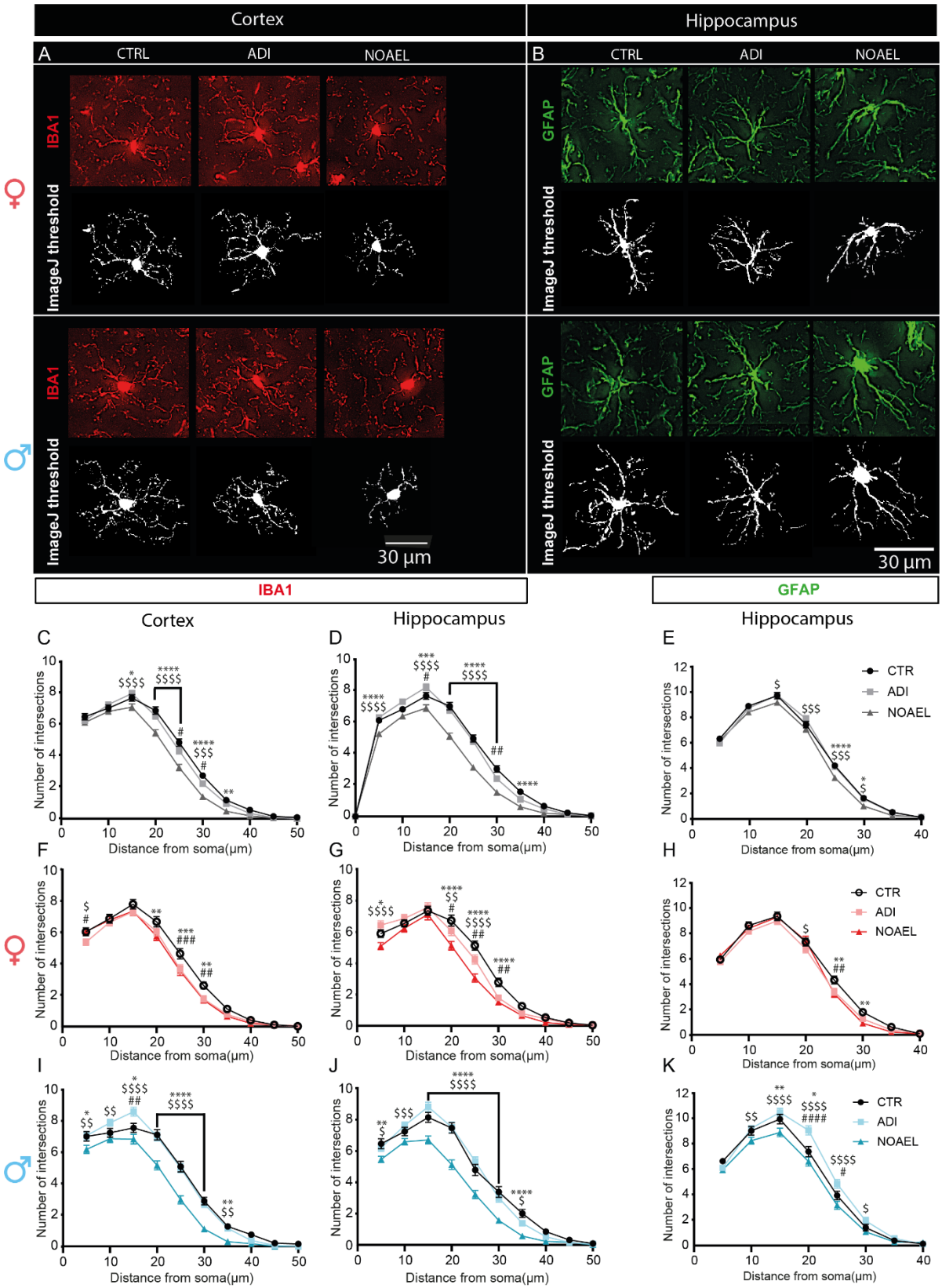

Figure 4. NOAEL glyphosate exposure associates with histological microglia modifications in the adult brain. (A) Representative images showing IBA1 immunofluorescence in the parietal cortex in female and male mice. **(B)** Representative images showing GFAP immunofluorescence in the hippocampus in female and male mice. The morphology of microglia (IBA1 staining and ImageJ threshold) was assessed using Sholl analysis in the parietal cortex and the hippocampus of CTR, ADI, and NOAEL groups.

Quantification of the sholl analysis in the parietal cortex **(C, F, and I)** and the hippocampus **(D, G, and J)** of CTR, ADI, and NOAEL females and males. Cortex: Males CTR, n=105 cells from 7 mice; ADI, n=120 cells from 8 mice; NOAEL, n=120 cells from 8 mice; Females CTR, n=120 cells from 8 mice; ADI, n=117 cells from 8 mice; NOAEL, n=120 cells from 8 mice. Two-way ANOVA (Males: $p<0.0001$; Females: $p<0.0001$; Males and Females: $p<0.0001$). Hippocampus: Males CTR, n=90 cells from 6 mice; ADI, n=119 cells from 8 mice; NOAEL, n=115 cells from 8 mice; Females CTR, n=120 cells from 8 mice; ADI, n=113 cells from 8 mice; NOAEL, n=120 cells from 8 mice. Two-way ANOVA (Males: $p<0.0001$; Females: $p<0.0001$; Males and Females: $p<0.0001$). The morphology of astrocytes (GFAP staining and ImageJ threshold) was assessed using Sholl analysis in the hippocampus of CTR, ADI, and NOAEL groups. Quantification of the sholl analysis in the hippocampus **(E)** of CTR, ADI, and NOAEL females **(H)** and males **(K)**. Hippocampus: Males CTR, n=75 cells from 4 mice; ADI, n=90 cells from 5 mice; NOAEL, n=90 cells from 5 mice; Females CTR, n=93 cells from 5 mice; ADI, n=113 cells from 6 mice; NOAEL, n=94 cells from 5 mice. Two-way ANOVA (Males: $p<0.0001$; Females: $p=0.0022$; Males and Females: $p<0.0001$). Asterisks indicate statistical significance (* $p < 0.05$; ** $p < 0.01$; *** $p < 0.001$; **** $p < 0.0001$); *: CTR vs NOAEL; $: ADI vs NOAEL; #: CTR vs ADI; ns: non-significative. Statistical significance was reported between genotype comparisons under each graphic.

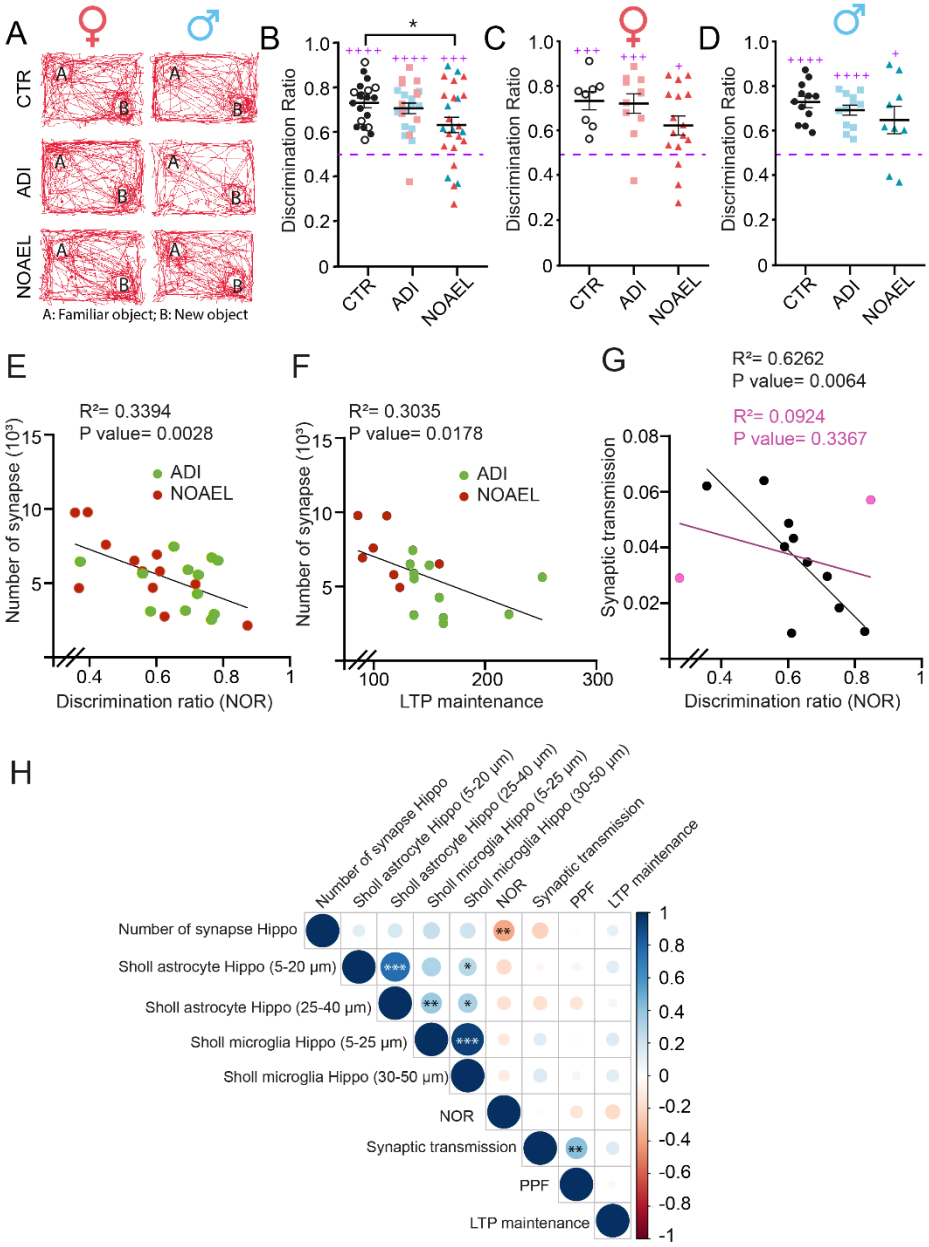

Figure 5. Mouse-specific cross-correlation of neurophysiological and histological data set. (A-D) 24 hours after the open field test, mice were exposed to two similar objects in the arena, and 24 hours later, one familiar object was replaced by a new one. The discrimination ratio was calculated, revealing a decrease in performance. Males CTR, n=12; ADI, n=12 ; NOAEL, n=9; Females CTR, n=8; ADI, N=11; NOAEL, n=16. One-way ANOVA test (Discrimination ratio Males: p=0.3232; Females: p=0.1502; Males + Females: p=0.041). Asterisks indicate statistical significance (* $p < 0.05$), and purple + symbols indicate statistical significance regarding the discrimination ratio value fixed at 0.5 (One sample t-test). **(E)** The number of synapses was correlated with the discrimination ratio obtained using the novel object recognition test. **(F)** The number of synapses was correlated with LTP maintenance. **(G)** The synaptic transmission was correlated with the discrimination ratio obtained using the novel object recognition test for female and male NOAEL. Pink simple linear regression showed non-significant R^2 and P values. Black simple linear regression was calculated by removing the two pink values from the analysis. **(H)** Correlation coefficients were calculated using the Pearson coefficients and considered statistically significant with *: R2>0.35, P<0.01; **: R2>0.4, P<0.001; ***: R2>0.5, P<0.00001. The areas of circles or squares show the absolute value of

corresponding correlation coefficients; the colors of circles show both the sign and the absolute value of the correlation coefficients.

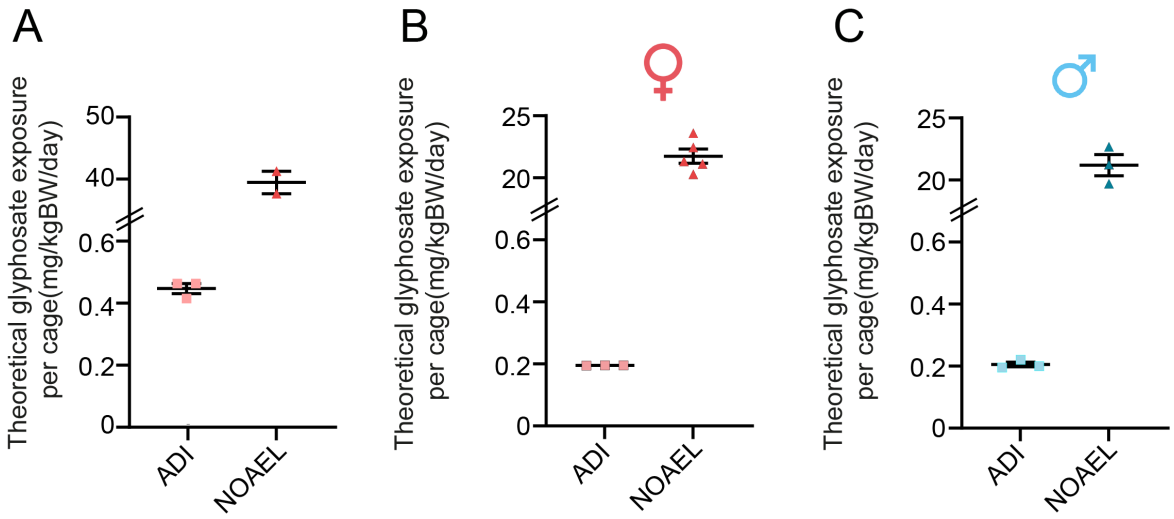

Supplemental Figure 1. Exposure of F0 dams **(A)** and F1 females **(B)** and males **(C)** was evaluated. The NOAEL dose corresponds to 100 times the ADI level.

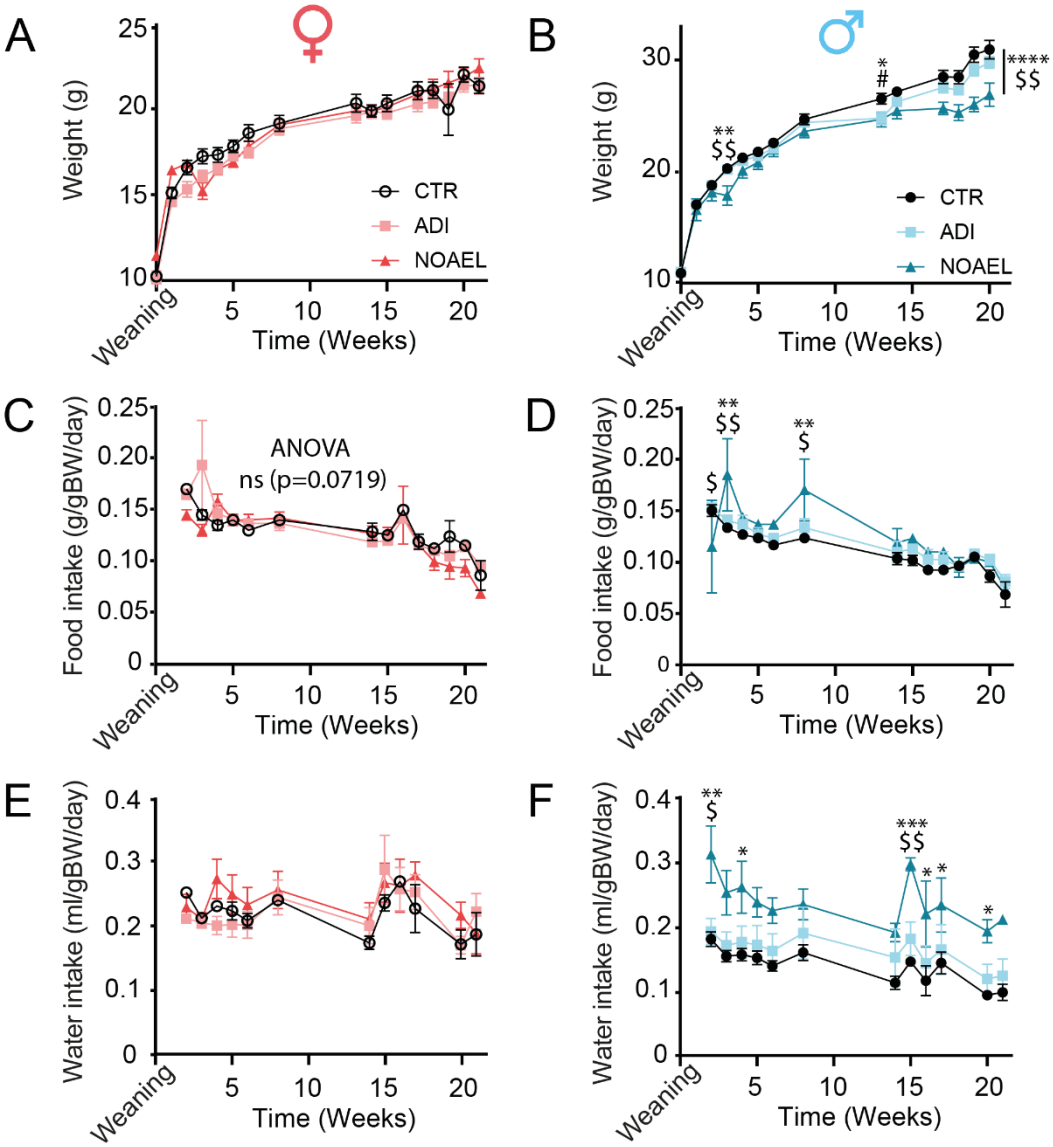

841

842 **Supplemental Figure 2. Weight gain, food, and water intake monitoring. (A-B)** Pups'
843 weight gain (grams), food **(C-D)**, and water intakes **(E-F)** expressed as g or ml/gram of body
844 weight (gBW)/day(d) were monitored from weaning. Males CTR, n=12 ; ADI, n=12 ; NOAEL,
845 n=9 ; Females CTR, n=8 ; ADI, n=11; NOAEL, n=16. Males: Two-way ANOVA test (weight
846 gain: $p<0.0001$; food intake: $p=0.0009$; water intake: $p<0.0001$); Females: Kruskal-Wallis
847 test (weight gain: $p=0.7546$) and two-way ANOVA test (food intake: $p=0.0719$; water intake:
848 $p=0.2042$). Asterisks indicate statistical significance (* $p < 0.05$; ** $p < 0.01$; *** $p < 0.001$; ****
849 $p < 0.0001$); *: CTR vs NOAEL; $: ADI vs NOAEL; #: CTR vs ADI; ns: non-significant. Statistical
850 significance was reported between genotype comparisons under each graphic.

851

852

853

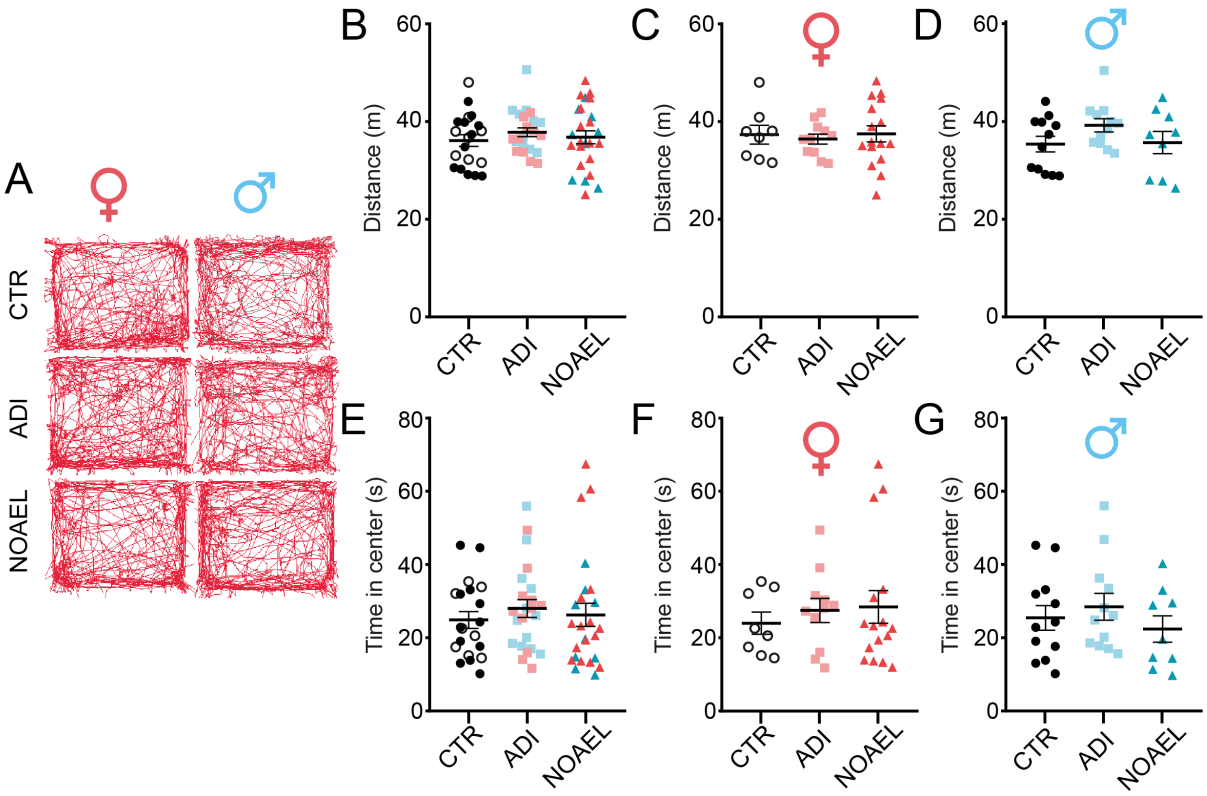

Suplemental Figure 3. Pre- and post-natal continuous glyphosate exposure and adulthood behavior screening. Mice were tested for the OF **(A).** The total distance traveled **(B-D)** and time spent in the center zone **(E-G)** were measured over 10 minutes. Males CTR, n=12; ADI, n=12 ; NOAEL, n=9 ; Females CTR, n=8 ; ADI, n=11 ; NOAEL, n=16. Males: One way ANOVA test (Distance: p=0.2085; Time spent in the center zone: p=0.5171); Females: One way ANOVA test (Distance: p=0.8771) and Kruskal-Wallis test (Time spent in the center zone: p=0.8258); Males and Females: One way ANOVA test (Distance: p=0.5969) and Kruskal-Wallis test (Time spent in the center zone: p=0.524).

		WT CTR		WT ADI		WT NOAEL		P value
		Mean	SEM of discrepancy	Mean	SEM of discrepancy	Mean	SEM of discrepancy	
NEUROTRANSMISSION	**Input/output test M**							
Fig. 1	*Shapiro-Wilk normality test M*	*yes*		*yes*		*yes*		
	Two-way ANOVA (group effect) M							*0,2748*
	Input/output test F							
	Shapiro-Wilk normality test F	*yes*		*yes*		*yes*		
	Two-way ANOVA (group effect) F							*0,1929*
	Input/output test M+F							
	Shapiro-Wilk normality test M+F	*yes*		*yes*		*yes*		
	Two-way ANOVA (group effect) M+F							*0,0074 ** *
	Paired pulse facilitation test M	**1,582 (N=12)**	**0,03019**	**1,498 (N=11)**	**0,03605**	**1,764 (N=6)**	**0,1372**	
	Shapiro-Wilk normality test M	*yes*		*yes*		*yes*		
	Ordinary one-way ANOVA M+F							*0,0236 * *
	Paired pulse facilitation test F	**1,549 (N=7)**	**0,04379**	**1,539 (N=9)**	**0,0525**	**1,662 (N=16)**	**0,03939**	
	Shapiro-Wilk normality test F	*yes*		*yes*		*yes*		
	Ordinary one-way ANOVA F							*0,0985*
	Paired pulse facilitation test M+F	**1,57 (N=19)**		**1,516 (N=20)**		**1,69 (N=22)**		
	Shapiro-Wilk normality test M+F	*yes*		*yes*		*yes*		
	Ordinary one-way ANOVA M+F							*0,0033 ** *
NEURONAL PLASTICITY	**Long-term potentiation maintenance test M**	**178,2 (N=10)**	**14,77**	**170,0 (N=10)**	**12,2**	**119,0 (N=7)**	**13,45**	
Fig. 2	*Shapiro-Wilk normality test M*	*no*		*yes*		*yes*		
	Kruskall-Wallis test M							*0,0109 * *
	Long-term potentiation maintenance test F	**146,7 (N=7)**	**12,9**	**151,0 (N=8)**	**6,112**	**127,8 (N=10)**	**8,495**	
	Shapiro-Wilk normality test F	*yes*		*yes*		*yes*		
	Ordinary one-way ANOVA F							*0,1657*
	Long-term potentiation maintenance test M+F	**162,0 (N=17)**	**9,933**	**164,3 (N=17)**	**7,555**	**121,8 (N=16)**	**7,424**	
	Shapiro-Wilk normality test M+F	*no*		*no*		*yes*		
	Kruskall-Wallis test M+F							*0,0003 *** *
SYNAPTIC DENSITY	**synaptic density M**	**4058 (N=6)**	**618,9**	**4868 (N=6)**	**444,4**	**5709 (N=6)**	**570,7**	
Fig. 3	*Shapiro-Wilk normality test M*	*yes*		*no*		*no*		
	Kruskall-Wallis test M							*0,0964*
	Synaptic density F	**4808 (N=6)**	**573,6**	**5214 (N=6)**	**572,9**	**6324 (N=6)**	**594,9**	
	Shapiro-Wilk normality test F	*yes*		*yes*		*yes*		
	Ordinary one-way ANOVA F							*0,1692*
	Synaptic density M+F	**4467(N=6)**	**419,7**	**5034(N=6)**	**355,8**	**6003 (N=6)**	**409,8**	
	Shapiro-Wilk normality test M+F	*no*		*yes*		*yes*		
	Kruskall-Wallis test M+F							*0,0243 * *
NEUROINFLAMMATION MICROGLIA CORTEX	**Sholl analysis M**	**(N=105)**		**(N=120)**		**(N=120)**		
Fig. 4	*Two-way ANOVA (group effect) M*							*<0,0001 **** *
	Sholl analysis F	**(N=120)**		**(N=117)**		**(N=120)**		
	Two-way ANOVA (group effect) F							*<0,0001 **** *
	Sholl analysis M+F	**(N=225)**		**(N=117)**		**(N=120)**		
	Two-way ANOVA (group effect) M+F							*<0,0001 **** *
NEUROINFLAMMATION MICROGLIA HIPPOCAMPUS	**Sholl analysis M**	**(N=90)**		**(N=119)**		**(N=115)**		
Fig. 4	*Two-way ANOVA (group effect) M*							*<0,0001 **** *
	Sholl analysis F	**(N=120)**		**(N=113)**		**(N=120)**		
	Two-way ANOVA (group effect) F							*<0,0001 **** *
	Sholl analysis M+F	**(N=168)**		**(N=203)**		**(N=184)**		
	Two-way ANOVA (group effect) M+F							*<0,0001 **** *
NEUROINFLAMMATION ASTROCYTE HIPPOCAMPUS	**Sholl analysis M**	**(N=75)**		**(N=90)**		**(N=90)**		
Fig. 4	*Two-way ANOVA (group effect) M*							*<0,0001 **** *
	Sholl analysis F	**(N=93)**		**(N=113)**		**(N=94)**		
	Two-way ANOVA (group effect) F							*0,0022 ** *
	Sholl analysis M+F	**(N=168)**		**(N=203)**		**(N=184)**		
	Two-way ANOVA (group effect) M+F							*<0,0001 **** *
BEHAVIOR	**Open field distance (cm) M**	**3537 (N=12)**	**160,7**	**3921 (N=12)**	**134,4**	**2639 (N=9)**	**227,9**	
Fig. 5 and supplemental figure 3	*Shapiro-Wilk normality test M*	*yes*		*yes*		*yes*		
	Ordinary one-way ANOVA M							*0,2085*
	Open field distance (cm) F	**3154 (N=8)**	**191,9**	**3139 (N=11)**	**104**	**2492 (N=16)**	**165,6**	
	Shapiro-Wilk normality test F	*yes*		*yes*		*yes*		
	Ordinary one-way ANOVA							*0,8771*
	Open field distance (cm) M+F	*3613 (N=20)*	*121,9*	*3784 (N=23)*	*89,37*	*3681 (N=25)*	*132,2*	
	Shapiro-Wilk normality test M+F	*yes*		*yes*		*yes*		
	Ordinary one-way ANOVA							*0,5969*
	Open field time in center (s) M	**25,47 (N=12)**	**3,373**	**28,49 (N=12)**	**3,672**	**22,44 (N=9)**	**3,607**	
	Shapiro-Wilk normality test M	*yes*		*yes*		*yes*		
	Ordinary one-way ANOVA M							*0,5171*
	Open field time in center F	**23,99 (N=8)**	**3,039**	**27,48 (N=11)**	**3,311**	**28,41 (N=16)**	**4,462**	
	Shapiro-Wilk normality test F	*yes*		*yes*		*no*		
	Kruskall-Wallis test F							*0,8258*
	Open field time in center M+F	**24,88 (N=20)**	**2,311**	**28,01 (N=23)**	**2,432**	**26,26 (N=25)**	**3,141**	
	Shapiro-Wilk normality test M+F	*yes*		*yes*		*no*		
	Kruskall-Wallis test M+F							*0,524*
	Discrimination ratio M	**0,7286 (N=12)**	**0,02573**	**0,692 (N=12)**	**0,02257**	**0,6479 (N=9)**	**0,06177**	
	Shapiro-Wilk normality test M	*yes*		*yes*		*yes*		
	Ordinary one-way ANOVA M							*0,3232*
	Discrimination ratio F	**0,7332 (N=8)**	**0,04032**	**0,7214 (N=11)**	**0,04381**	**0,6225 (N=16)**	**0,04318**	
	Shapiro-Wilk normality test F	*yes*		*yes*		*yes*		
	Ordinary one-way ANOVA F							*0,1502*
	Discrimination ratio M+F	**0,7305 (N=20)**	**0,02167**	**0,7061 (N=23)**	**0,02366**	**0,6316 (N=25)**	**0,03478**	
	Shapiro-Wilk normality test M+F	*yes*		*yes*		*yes*		
	Ordinary one-way ANOVA M+F							*0,041 * *
PHYSIO PARAMETERS	**Weight gain (%) M**							
Supplemental figure 2	*Shapiro-Wilk normality test M*	*yes*		*yes*		*yes*		
	Two-way ANOVA (group effect) M							*0,0182 * *
	Weight gain (%) F							
	Shapiro-Wilk normality test F	*no*		*no*		*yes*		
	Kruskall-Wallis test F							*0,7546*
	Food intake (g/ kg bw/ d) M							
	Shapiro-Wilk normality test M	*yes*		*yes*		*yes*		
	Two-way ANOVA (group effect) M							*0,1705*
	Food intake (g/ kg bw/ d) F							
	Shapiro-Wilk normality test F	*yes*		*yes*		*yes*		
	Two-way ANOVA (group effect) F							*0,1229*
	Water intake (g/ kg bw/ d) M							
	Shapiro-Wilk normality test M	*yes*		*yes*		*yes*		
	Two-way ANOVA (group effect) M							*0,9994*
	Water intake (g/ kg bw/ d) F							
	Shapiro-Wilk normality test F	*yes*		*yes*		*yes*		
	Two-way ANOVA (group effect) F							*0,9957*

Supplemental Table 1. Summary of statistical analyses.